Mobility of oxygen vacancy in $SrTiO_3$ and its implications for oxygen-migration-based resistance switching

W. Jiang, M. Noman, Y. M. Lu, J. A. Bain, P. A Salvador, and M. Skowronski

Citation: Journal of Applied Physics **110**, 034509 (2011);
View online: https://doi.org/10.1063/1.3622623
View Table of Contents: http://aip.scitation.org/toc/jap/110/3
Published by the American Institute of Physics

Mobility of oxygen vacancy in $SrTiO_3$ and its implications for oxygen-migration-based resistance switching

W. Jiang,[1,a)] M. Noman,[2] Y. M. Lu,[1] J. A. Bain,[2] P. A Salvador,[1] and M. Skowronski[1]
[1]*Materials Science and Engineering Department, Carnegie Mellon University, 5000 Forbes Ave., Pittsburgh, Pennsylvania 15213, USA*
[2]*Electrical and Computer Engineering Department, Carnegie Mellon University, 5000 Forbes Ave., Pittsburgh, Pennsylvania 15213, USA*

(Received 25 January 2011; accepted 1 July 2011; published online 9 August 2011)

Capacitance−voltage characteristics of high quality Pt Schottky diodes fabricated on oxygen-vacancy-doped $SrTiO_3$ single crystals were used to obtain the oxygen vacancy profiles within one microns of the Pt interface. Computer simulations based on solving the drift-diffusion equations for electrons and ionized vacancies were performed to understand the experimentally observed oxygen vacancy profile's time-evolution at room temperature and 0 V applied bias. Building upon this understanding, the diode's room temperature profile evolution under −35 V applied bias was analyzed to yield a vacancy mobility value of 1.5×10^{-13} $cm^2/V{\cdot}s$ at an electric field of 500 kV/cm. This mobility is 8 orders of magnitude too low to produce nanosecond resistance switching in thin film devices. The applicability of the results to oxygen-migration-based resistance switching is discussed relative to recent observations and modeling. © *2011 American Institute of Physics*. [doi:10.1063/1.3622623]

I. INTRODUCTION

Interest in the resistance switching (RS) of metal/oxide/metal structures has surged in the past decade owing to its promise in the next generation data storage technology.[1–5] Among the various models proposed for RS, the oxygen-migration-based model has attracted a great deal of attention due to its success in describing the behaviors of the Pt/TiO_{2-x}/Pt RS system.[6–11] Oxygen vacancies in many oxides behave as mobile donors[12–14] and, as a consequence, their concentration at the metal/oxide interface can be controlled electrically. For a Schottky interface, such as Pt/TiO_{2-x}, a sufficiently strong electric field can induce a vacancy concentration buildup or depletion at the interface, resulting in the change of the effective Schottky barrier height. In boundary cases, the device's current−voltage ($I-V$) characteristic can switch from that of a rectifier to a linear resistor.[7,15] The factors limiting the use of oxygen-migration-based RS devices for data storage are the switching speed, endurance and the retention time. Experimentally, a fast switching time (<100 ns) and a high endurance (>10^7 read/write cycles) have been demonstrated[7,16–18] but only few reports focus on the retention time.[16,17] The kinetic requirement for fast switching (high vacancy mobility) and long retention (low vacancy mobility) presents the so called "voltage-time" dilemma.[19] Noman *et al.*[20] addressed this dilemma through modeling and found that, by using standard drift and diffusion equations with an electric-field-dependent vacancy mobility and local heating, no realistic operating window exists where the device can both switch in nanoseconds and have a 10 year retention.

In this work, we address the "voltage-time" dilemma experimentally by examining the near-interface oxygen vacancy motion in the Pt/$SrTiO_{3-x}$ Schottky diode using a capacitance−voltage ($C-V$) technique. $SrTiO_3$ is a known RS oxide[16,21,22] that is electrically similar to TiO_2, but does not readily form an oxygen deficient second phase (such as the Magnéli phases in TiO_2). In this sense, $SrTiO_3$ relates more closely to the model system where only drift and diffusion control the vacancy concentration. The study of vacancy motion by $C-V$ offers three advantages over other techniques (such as $I-V$ or electrocoloration[13]). First, under reverse bias, the electrons are blocked at the interface. High electric fields can be applied across the depletion layer with minimum current flow, thus avoiding local Joule heating. Second, quantitative and direct information about the charge distribution near the interface can be obtained from straightforward analysis of the diode's $C-V$ characteristics with the resolution much higher than in electrocoloration. Third, since capacitance is proportional to contact area, the $C-V$ behavior is insensitive to lateral inhomogeneities such as dislocations and grain boundaries that can dominate $I-V$ characteristics. Using these advantages, we determine the oxygen vacancy profile from $C-V$ measurements on Pt/$SrTiO_{3-x}$ Schottky diodes and calculate the oxygen vacancy mobility from the time-evolution of the profiles at room temperature. The extracted values of mobility are discussed in the context of the RS "voltage-time" dilemma.

II. EXPERIMENT

To fabricate high quality, low leakage Pt/$SrTiO_{3-x}$ diodes, a standard surface cleaning technique,[23] consisting of a 45 s BHF etch and a 1000 °C air anneal, was first applied to undoped, one-side polished $SrTiO_3$ (001) single crystals (Crystal GmbH, Germany). Following the air anneal, a 250 nm thick Ti film was sputtered on the unpolished side of the crystal to serve both as the ohmic contact and as an

a) Electronic mail: wenkan@cmu.edu

oxygen getter.[24] The sample was then transferred to a high vacuum chamber (2×10^{-8} Torr) and annealed for 90 min at 400 °C. The annealing process changed the originally insulating, transparent crystal into a conductive, dark-blue colored one, presumably due to reaction between oxygen ions from the $SrTiO_3$ and Ti metal. Finally, 50 nm thick and 500 μm diameter wide Pt contacts were sputtered (RF sputtering at 5 mTorr Ar and 50 W power) through a shadow mask on the polished side of $SrTiO_{3-x}$. A similar procedure, minus the reduction step, was used to fabricate Pt Schottky contacts on a 0.01 wt. % Nb:$SrTiO_3$ control sample (Crystal GmbH, Germany). Both the Nb dopants and oxygen vacancies are shallow donors in $SrTiO_3$ with the major difference being ion mobility; Nb^{5+} can be considered as immobile.

All electrical biases were applied to the Pt top electrodes with the Ti back contact maintained at ground. $I-V$ measurements of the diodes were carried out with an Agilent Parameter Analyzer 4155 C (Santa Clara, CA), using a double sweep starting from negative bias with steps of 0.1 V. $C-V$ measurements were carried out with a HP LF Impedance Analyzer 4192 A, using a single sweep starting from positive bias with an oscillation frequency of 10 kHz, oscillation amplitude of 5 mV, and a step of 0.1 V.

III. RESULTS AND DISCUSSION

Figures 1(a) and (b) show the typical $J-V$ characteristics (plotted as the absolute value of current density) for the Pt/Nb:$SrTiO_3$ and Pt/$SrTiO_{3-x}$ diodes, respectively, immediately after fabrication. Both diodes are highly rectifying (leakage currents below measurement detection limit of 10 pA) with exponentially increasing forward bias currents

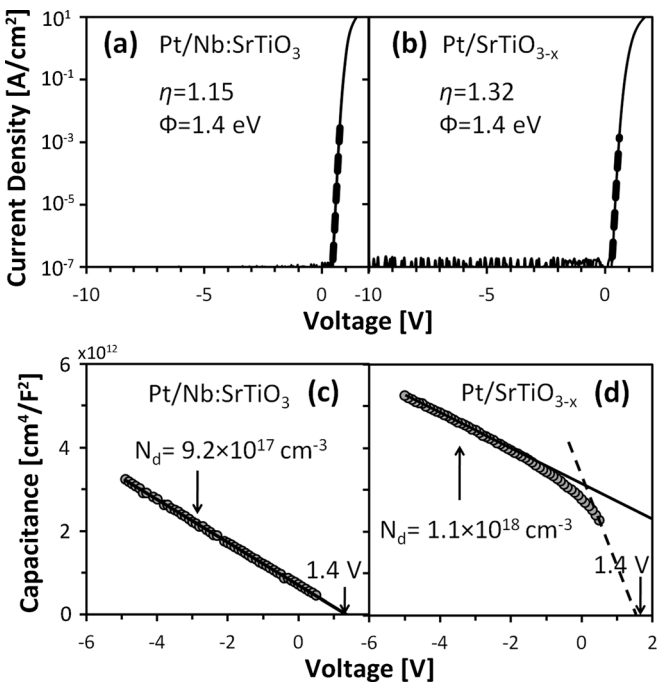

FIG. 1. (a) and (b) Compare the $J-V$ characteristics (measured from −10 to 5 to −10 V) of the as-fabricated Pt/Nb:$SrTiO_3$ and Pt/$SrTiO_{3-x}$ Schottky diodes, respectively. Exponential fits (thickened dotted line) to the forward bias part of each $J-V$ were used to determine ideality factors η and barrier heights Φ. (c) and (d) Compare the $1/C^2-V$ behaviors of the two diodes.

that were fitted with the thermionic emission equation (broad dotted line in the figures):[25]

$$J = A^* T^2 \exp\left(-\frac{q\Phi}{\eta\kappa \mathrm{T}}\right) \exp\left(\frac{qV}{\eta\kappa \mathrm{T}}\right), \tag{1}$$

where A^* is the Richardson constant, T the temperature, k the Boltzmann constant, Φ the Schottky barrier height, and η the ideality factor. Using 156 ($A/cm^2/K^2$) for A^*,[26] the estimated values for η and Φ were 1.15 and 1.4 eV for Pt/Nb:$SrTiO_3$ and 1.32 and 1.4 eV for Pt/$SrTiO_{3-x}$ diodes. These values are close to each other and to those reported for high quality Schottky diodes on $SrTiO_3$.[26] No RS-type hysteresis was observed during the $I-V$ sweep, which took approximately 5 s. The reason for the apparent lack of hysteresis is discussed later.

The C-V characteristics of the Pt/Nb:$SrTiO_3$ and Pt/$SrTiO_{3-x}$ diodes in their as-fabricated states are given in Fig. 1(c) and (d), plotted as $1/C^2$ vs V. The Pt/Nb:$SrTiO_3$ diode has a linear $1/C^2$ vs V with a voltage intercept of 1.4 V, which corresponds to a built-in potential of 1.4 eV. Adding the difference between the Fermi level (E_F) and the conduction bandedge of $SrTiO_3$ (E_C) to the built-in potential gives the Schottky barrier height. For a semiconductor with 10^{18} cm^{-3} donors at room temperature, E_C-E_F is ~0.1 eV. The small discrepancy in the Pt/Nb:$SrTO_3$ diode's Schottky barrier height obtained from $C-V$ and $I-V$ can be accounted for by nonideal factors such as image force lowering unique to the $I-V$ measurement. Unlike the Pt/Nb:$SrTiO_3$ diode, the $1/C^2$ vs V plot for the Pt/$SrTiO_{3-x}$ [Fig. 1(d)] cannot be fitted with a line. It consists of roughly a linear high-voltage region (−5 to −2 V) and a nonlinear low-voltage region (from −2 to 0.5 V). Linear extrapolation of the high-voltage data yielded a voltage intercept greater than 10 V. This value far exceeds any realistic built-in potential. However, an intercept of 1.4 V can be obtained by extrapolating the first few data points in the low voltage region as shown by the dotted line in Fig. 1(d). Such behavior is indicative of a depth-dependent charge density in the depletion region.

According to Schottky theory, the donor concentration N_d is inversely proportional to the derivative of the $1/C^2$ vs V via:[25]

$$\frac{d(1/C^2)}{dV} = \frac{2}{\varepsilon\varepsilon_o q N_d(W)}, \tag{2}$$

where ε is the dielectric constant of $SrTiO_3$ (300 at room temperature[27]), ε_o the permittivity of free space, q the electron charge, and W is the position of the depletion edge relative to the Schottky interface. The depletion edge position W is pushed deeper into the diode as the reverse bias V is increased. From the measured capacitance, the applied bias V can be converted to W via:

$$W(V) = \frac{\varepsilon\varepsilon_o}{C(V)} \tag{3}$$

These two equations allow for plotting the donor depth profile $N_d(x)$. For the Pt/Nb:$SrTiO_3$, the linear $1/C^2$ vs V relation gives a uniform donor profile with a concentration of

9.2×10^{17} cm^{-3}. For the Pt/$SrTiO_{3-x}$ diode, the $1/C^2$ vs V relation is linear only in the high-voltage region (−2 to −5 V), indicating a uniform donor concentration in the bulk of the sample, away from the Pt interface. This concentration was calculated to be 1.1×10^{18} cm^{-3}, a value similar to that of the Pt/Nb:$SrTiO_3$ diode. A highly nonlinear behavior is observed for the $1/C^2$ vs V relation in the low voltage region (−2 to + 0.5 V). Its local slope continually increases as the voltage approaches + 0.5 V, which implies that the donor concentration monotonically decreases from the bulk value toward the Pt interface. The reason for the donor-denuded zone close to the Pt/$SrTiO_{3-x}$ interface is discussed along with the time-evolution of the diode's $1/C^2$ vs V relation.

In these initial measurements, other than the low-voltage nonlinearity of the $1/C^2$ vs V, the Pt/$SrTiO_{3-x}$ diode with mobile donors is electrically similar to the Pt/Nb:$SrTiO_3$ control device. Differences arise in each diode's response to thermal and electrical stresses. The Pt/Nb:$SrTiO_3$ diode's electrical properties are completely insensitive to the applied stresses, which included annealing in air at 500 K for 3 h and stressing at −35 V for 24 h. This is an expected result as the Nb^{5+} dopant is immobile at these temperatures and electric fields. However, oxygen vacancy is sufficiently mobile even at room temperature to result in noticeable changes. As shown in Fig. 2(a), keeping the Pt/$SrTiO_{3-x}$ diode in air at room temperature (300 K) for 66 h led to a large upward shift of the $1/C^2$ vs V over the "initial" plot. This shift is due primarily to the increase in slope of the low-voltage region (−2 to 0.5 V), suggesting a further depletion of vacancies near the interface. Thermal activation is one characteristics of ion motion. To verify that the shifts in $1/C^2$ vs V share this

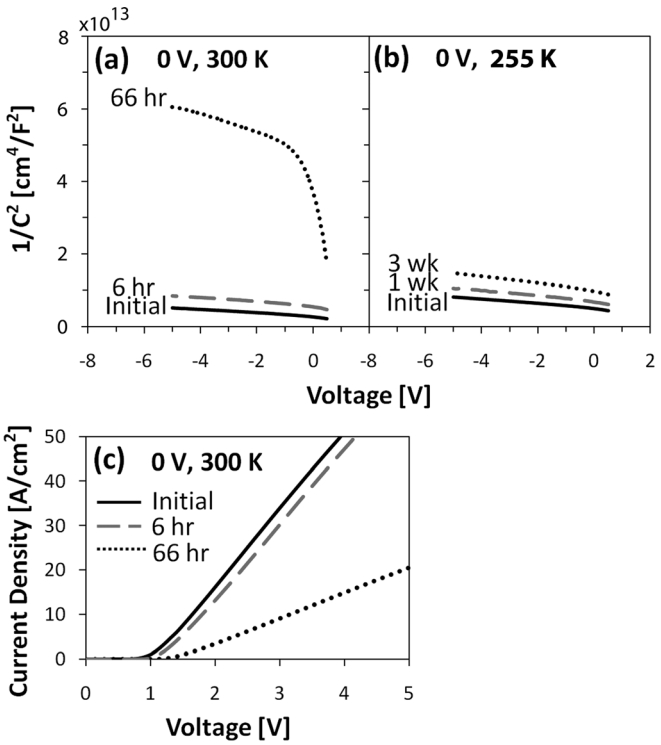

FIG. 2. (a) and (b) Time evolutions of the $1/C^2$ vs V behaviors of Pt/$SrTiO_{3-x}$ Schottky diodes at two temperatures with no applied bias. The evolution rate is significantly slower at 255 K. (c) Time evolution of the $J-V$ characteristic of Pt/$SrTiO_{3-x}$ Schottky diode at 300 K with no applied bias.

characteristic, a Pt/$SrTiO_{3-x}$ sample was placed in a standard freezer (255 °C) and the $C-V$ were periodically recorded at room temperature as shown in Fig. 2(b). Owing to the difference in elapsed time between sample fabrication and first measurement, which can be several hours, the initial states of the $C-V$ characteristics in Fig. 2(a) and 2(b) were somewhat different. Comparison of Fig. 2(a) and 2(b) shows that lowering the ambient temperature to 255 K slowed substantially the rate of the $1/C^2$ vs V's upward shift. After 3 weeks in air at 255 K, the change is similar to the change after 6 h at 300 K.

Figure 2(c) shows the time-evolution of the forward bias $J-V$ characteristics of Pt/$SrTiO_{3-x}$ diode at 300 K. At voltages in excess of the Schottky built-in voltage (1.4 V), the current is limited by the ohmic resistance of the neutral bulk $SrTiO_{3-x}$. The $J-V$ characteristics in this voltage region behaved linearly as expected with the current density decreasing over time. For example, the current density at 4 V decreased from 50 A/cm^2 to 15 A/cm^2 66 h after the initial measurement. This decrease in current density, which translates to an increase in the series resistance, along with the changes observed in $1/C^2$ vs V are consistent with the widening of a vacancy-denuded layer located close to the Pt/$SrTiO_{3-x}$ interface. Such electrical behavior might appear surprising as the electric field in the Schottky depletion region would exert the force in the direction of the interface on positively charged oxygen vacancies. An increase in vacancy concentration near the interface would result rather than the observed reduction. The vacancy buildup should continue with time until the diffusion due to steep concentration gradient would balance the drift of vacancies. At steady state, the concentration profile corresponds to a monotonic increase of the vacancy concentration toward the interface in accordance with Guoy-Chapman formula.[28] However, such steady state was never reached for the Pt/$SrTiO_{3-x}$ diode in the time scale of this experiment. The observed reduction of the vacancy concentration at the near interface region could be a transient phenomenon discussed below.

Let us assume that a Pt Schottky barrier is initially formed on a uniformly vacancy doped $SrTiO_{3-x}$. Also, let us assume that the interface is perfectly blocking, i.e., does not allow for the oxygen exchange. At the moment of diode formation, the electrons will be swept away from the interface, forming a Schottky depletion region with its associated internal electric field. The positively charged vacancies inside the depletion region will experience a force exerted by the electric field and will drift toward the Pt interface. However, the drift velocities will depend on position in the depletion layer as the field in a Schottky barrier is monotonically increasing toward the interface. The vacancies closer to the edge of the depletion (low field) will move more slowly compared to the ones closer to the Schottky interface (high field). The difference in drift velocity produces a flux gradient that reduces the vacancy concentration through most of the depletion region. At the same time, a pile-up of vacancy should occur right next to the Pt interface to conserve the net amount of oxygen vacancies. If such pile-up was to occur, $C-V$ could not capture it due to its limited range. Only the region away from the interface corresponding to reduced vacancy

concentration can be recorded, resulting in the impression of an interface oxidation.

This qualitative description was supported by the results of the simulation using model developed by Noman *et al.*[20] The model assumed that the Pt electrode completely blocks the exchange of outside oxygen with the vacancies in $SrTiO_{3-x}$. The built-in potential of the Schottky barrier was set to 1.55 eV with the maximum allowable concentration at the Pt interface equal to 2×10^{20} cm^{-3}. The initial state of the donor profile was set to be uniform with a concentration of 10^{18} cm^{-3}. The profile's time-evolution under the internal electric field of the Schottky barrier (no bias applied) is shown in Fig. 3(a), which contains four snapshots of donor profiles taken at time $t = \tau$, 10τ, 100τ, and 500τ. The time parameter τ is directly related to the activation energy for donor motion. Activation energy of 0.7 eV gives a τ of 5 min. The simulated profiles are in agreement with the qualitative description in the previous paragraph. For example, the profile at 500τ shows that a vacancy pile-up occurred at the interface, followed by a much wider depression with the minimum concentration of 2×10^{16} cm^{-3} at 0.02 μm away from the interface. The concentration gradually returns to the bulk value almost 2.5 μm deeper into the crystal. The arrows in Fig. 3(a) indicate the locations at which the concentration recovers to the bulk value. This location recedes from the Pt interface together with the vacancy concentration at the local minimum decreasing over time. The inset of Fig. 3(a) shows the details of the pile-up at time interval of τ, 10τ, and 500τ.

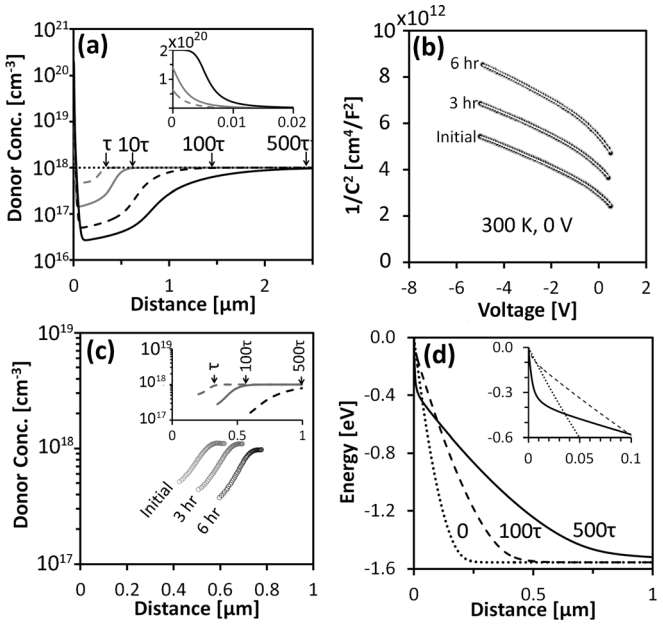

FIG. 3. (a) Simulated time-evolution of an initially uniform donor profile under no applied bias with concentration plotted in log scale. The inset is the zoomed-in view of the pile-up at the interface with concentration plotted in linear scale. (b) Experimentally measured room temperature $1/C^2$ vs V evolution of a Pt/$SrTiO_{3-x}$ diode under no applied bias. (c) Donor profiles corresponding to the $1/C^2$ vs V evolution. The inset of (c) is the simulated donor profile evolution shown in (a) but with the interface region truncated. (d) Schottky barrier's potential energy evolution corresponding to the simulated donor profile evolution in (a). The inset zooms in on potential energy profile within 100 nm of the interface. In all figures, the axes of the inset and the main image have the same units.

The axes of the inset have the same unit as the main with the y-axis plotted in linear scale. After 500τ, the pile-up region is still confined to ~10 nm of the interface, a region inaccessible by $C-V$ profiling.

Figure 3(b) shows the room temperature $C-V$ evolution of a Pt/$SrTiO_{3-x}$ diode under 0 V applied bias taken at three different times ("initial," "3 h," and "6 h"). The "initial" $C-V$ measurements were typically taken a few hours after Pt deposition. The $1/C^2$ vs V plot shifts upward over time while its high voltage slope (−2 to −5 V) remains unchanged. To construct the donor profiles, each plot in Fig. 3(b) was fitted with a fourth degree polynomial (shown in the figure as solid white lines with the actual data points represented as dark thicker line in the background). Equation (2) was applied to the derivative of the polynomial to find the donor concentration corresponding to each measurement voltage. Equation (3) was used to convert the measurement voltages to positions inside $SrTiO_{3-x}$. Resulting donor profiles are plotted in Fig. 3(c) on the logarithmic scale. The "initial," "3 h," and "6 h" profiles all show a plateau in concentration at a value of $\sim 1 \times 10^{18}$ cm^{-3}. The position at which the vacancy concentration begins to decrease from the plateau moves deeper into the $SrTiO_{3-x}$, a feature also observed in the simulation. This motion of the donor profiles away from Pt/$SrTiO_{3-x}$ interface corresponds to the upward motion of $1/C^2$ vs V plots in Fig. 3(b). Owing to the limited range of $C-V$, only donor profile ~400 nm or further away from the Pt interface could be probed experimentally in this diode. The inset of Fig. 3(c) plots a portion of the simulated donor profile evolution in Fig. 3(a) excluding the pile-up at the interface. The x and y axes are the same for both the inset and the main plot. Comparison of the simulated and experimentally obtained profiles in Fig. 3(c) shows them to be qualitatively similar. Whether or not a pile-up occurred at the Pt interface cannot be determined by $C-V$ measurement.

One important assumption made in the simulation is that the Pt electrode is perfectly blocking, sealing the system off from exchange with outside oxygen. If this is not the case, an oxidation of the interface instead of a pile-up could result and $C-V$ would be unable to distinguish the difference. The vacuum reduction process of $SrTiO_3$ is expected to establish a uniform oxygen vacancy concentration throughout the crystal. When cooled to room temperature and exposed to air, the crystal will slowly oxidize as its vacancy concentration is far in excess of the equilibrium value. The oxidation process will start at the sample surface via the following oxygen incorporation reaction:

$$\frac{1}{2}O_2 + V_{\ddot{o}} + 2e' \rightarrow O_o^{\times} \tag{4}$$

If this reaction proceeds faster than the drift and diffusion of oxygen vacancies toward the interface, a vacancy-denuded layer will be created with a real concentration minimum at the interface (unlike in the simulation where the minimum was local and existed next to a pile-up). One mechanism that would act as a source for oxygen (or sink for vacancies) is the dissociation of atmospheric oxygen and its diffusion

through the 50 nm thick Pt contact. However, when the diode was maintained in a 2×10^{-8} Torr vacuum immediately after fabrication, the vacancy profile continued to shift rightward at the same rate as before (as measured by $C-V$). This suggests that the source of oxygen (if there is a source) is likely a preexisting adsorbed layer of oxygen on the $SrTiO_{3-x}$ surface prior to the deposition of Pt electrodes and dissolved in the Pt electrode during deposition, as the sample was exposed to air while being transferred to the sputtering chamber. Pt is a known oxygen dissociation catalyst[29] and it is reasonable to assume that adsorbed molecular oxygen dissociated quickly during Pt deposition (during which the $SrTiO_{3-x}$ surface can also be heated considerably[30]). The dissociated oxygen then exchanges with the oxygen vacancies close to the Pt/$SrTiO_{3-x}$ interface via Eq. (4), resulting in the initial interface-denuded dopant profile and the subsequent continued expansion of the denuded-zone observed in $C-V$. It is worth noting that a monolayer coverage of oxygen on the $SrTiO_{3-x}$ surface is enough to completely oxidize 6 μm thick layer of $SrTiO_{3-x}$ that has a vacancy concentration of 1×10^{18} cm^{-3}.

One electrical characteristics sensitive to the interface donor concentration is the reverse bias leakage current. If an oxygen vacancy pile-up occurred at the Pt interface, the Schottky barrier width will be reduced at the interface, allowing tunneling through the barrier to occur more easily. However, because of the large barrier height of the Pt/$SrTiO_{3-x}$ diode ($\sim$1.5 V) and the high dielectric permittivity of $SrTiO_3$ (300 at room temperature),[27,31] a significant pile-up would be required before the effect of barrier thinning becomes noticeable. The 0 bias potential evolution corresponding to the simulated donor profiles in Fig. 3(a) at time $t=0$, 10τ, and 500τ are shown in Fig. 3(d). The depletion edge of the potential profile at $t=0$, which corresponds to a uniform donor profile with $N_d = 10^{18}$/cm^3 is at approximately 250 nm. The depletion edge moves deeper into the sample over time. At 500τ, the edge is at approximately 1 μm away from the Pt interface. Despite the pile-up at the interface, which thinned the Schottky barrier in that region, the overall depletion width is widened by the donor-denuded zone next to the pile-up. This increase in depletion width let to a drop in the measured capacitance, which shifted upward the $1/C^2$ vs V plot. The inset of Fig. 3(d) is an expanded view of the potential profile close to the Pt/$SrTiO_{3-x}$ interface. The x and y axes have the same units as the main image. Owing to the pile-up at the interface after 500τ, the potential energy dropped by 0.3 eV in a distance of only 5 nm. The same potential drop occurred over a distance of $\sim$25 nm in the initial ($t=0$) profile. $I-V$ simulation (not shown) suggests that electron can tunnel through 5 nm of the Pt/$SrTiO_{3-x}$ barrier easily, which means that the effective Schottky barrier height of the device after 500τ is lowered by 0.3 eV. However, the build-in potential is 1.55 eV in the simulation. The tunneling current through an effective Schottky barrier of 1.25 eV is still below the measurable limit experimentally. A much more significant pile-up is needed before one can experimentally assess the reverse-bias leakage current of the Pt/$SrTiO_{3-x}$ diode due to barrier-thinning.

Both interface oxidation and pile-up can produced a profile evolution shown in Fig. 3(c). Further investigation is needed to determine whether oxidation or pile-up or a combination of both occurred at the interface. However, the vacancy mobility under a large electric field comparable in strength to that of the typical switching field can still be studied regardless of the state of the interface. Figure 4(a) is the $1/C^2$ vs V plots for a Pt/$SrTiO_{3-x}$ diode measured initially, 5 and 20 min after electrical stressing under -35 V at room temperature. All three plots can be roughly broken into the nonlinear low voltage region (-0.5 to -2 V) and the linear high-voltage region (-2 to -5 V). Similar to the $C-V$ evolution with no applied bias [Fig. 3(b)], the $1/C^2$ vs V plots shifted upward with time under -35 V bias. However, whereas the upward shift in the 0 bias case is limited to only changes in local slope in the low voltage region (0.5 to -2 V), the slopes of the entire voltage range (0.5 to -5 V) was increased under the -35 V bias. Figure 4(b) shows the time evolution of the donor profiles corresponding to the $1/C^2$ vs V plots in Fig. 4(a). Not only did the donor profiles move rightward away from the Pt interface with time, but the concentration plateau also shifted downward from 1.1×10^{18} cm^{-3} to 5×10^{17} cm^{-3} over 20 min. This downward shift of the plateau is absent in the 0 bias profile evolution [Fig. 3(c)] and is associated with the high-voltage slope increase of the $1/C^2$ vs V plots. The accelerated rate of rightward shift under -35 V bias relative to the rate under 0 bias was expected since the reverse bias drives oxygen vacancy in the same direction as the internal electric field of the Schottky barrier. The reason for the additional downward shift of the concentration plateau can be explained by using

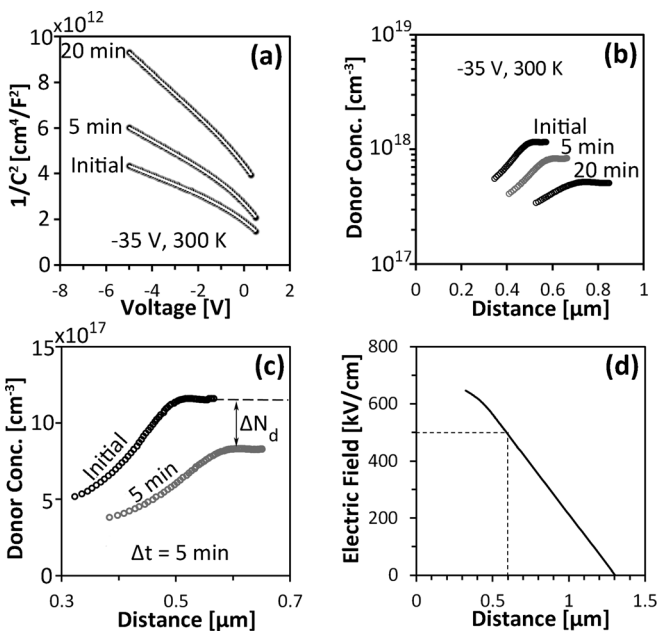

FIG. 4. (a) Plots the room temperature $1/C^2$ vs V evolution of a Pt/$SrTiO_{3-x}$ diode under -35 V bias. (b) Plots the corresponding donor profiles obtained from (a) with concentration in logarithmic scale. (c) Focuses on the "Initial" and "5 min" profiles shown in (a) with the concentration plotted in linear scale. (d) Electric field profile obtained from the "Initial" donor profile in (b) with the assumption that the plateau region extends to the edge of depletion at -35 V.

the standard drift and diffusion mechanisms. The vacancy profiles in both Fig. 3(c) and Fig. 4(b) were obtained from $C-V$ measured between $+0.5$ and -5 V. As discussed above, the depletion edge position is directly related to applied bias via Eq. (3). The greater the reverse bias magnitude, the deeper the edge extends into the sample. Outside the depletion layer, the electric field is zero. With no bias applied, only the internal electric field of the Schottky barrier acts on the diode. The $C-V$ characteristics measured in the voltage range between 0 and -5 V (and the corresponding donor profile) lie outside the influence of the internal electric field and evolved primarily due to diffusion. Since the diffusive flux vanishes in the concentration plateaus of Fig. 3(c), where the concentration gradient $dN_d/dx = 0$, only a rightward shift in vacancy profile was observed.

Under -35 V, the depletion edge position extends well beyond that at -5 V, which means that the entire profile shown in Fig. 4(b) evolved under the influence of an electric field whose field gradient dE/dx is described by the Poisson's equation [Eq. (5)].[25]

$$\frac{dE(x)}{dx} = -\frac{qN_d}{\varepsilon\varepsilon_o} \tag{5}$$

The presence of a field gradient translates to a vacancy flux gradient via Eq. (6)

$$\frac{dJ_{\text{drift}}}{dx} = \mu_v N_d \frac{dE}{dx}, \tag{6}$$

where μ_v is the vacancy mobility. This flux gradient is negative following the sign of the field gradient. A reduction of vacancy concentration occurred as a result of the negative field gradient, similar to the process that created the donor-denuded zone in the simulation [Fig. 3(a)]. It is interesting to note that according to Eq. (5) and Eq. (6), a constant donor concentration in the plateau region produces a constant flux gradient. This is the reason why the plateau in Fig. 4(b) is uniformly lowered by the -35 V stressing.

Oxygen vacancy mobility was estimated by calculating the time needed to lower the plateau from one concentration value to another. Since the downward movement of the concentration plateau in Fig. 4(b) is a feature associated with drift (as discussed above), limiting the analysis to this feature allows the use of Fick's second law in the form:

$$\frac{qN_d}{dt} = \frac{dJ_{\text{drift}}}{dx} = \mu_v N_d \frac{dE}{dx} \tag{7}$$

The dN_d/dt term in the equation can be approximated as $\Delta N_d/\Delta t$ and calculated from profiles taken at two different times. Figure 4(c) demonstrates the calculation using the "initial" and "5 min" donor profiles in Fig. 4(b). A linear scale is used for the y axis. ΔN_d is calculated by taking the difference between the donor concentrations at the two plateau regions as indicated by the vertical double arrow. The N_d term in Eq. (7) is approximated as the average of the two concentrations at the plateaus. An oxygen vacancy mobility of 1.5×10^{-13} cm^2/V·s was calculated from this analysis.

To estimate the electric field under which the mobility value is obtained, an integration of the Poisson's equation using the "initial" donor profile in Fig. 4(c) starting from the edge of t -35 V up to the position of interest is needed. Applying Eq. (3) to the capacitance value at -35 V yielded a depletion edge position of 1.2 μm away from the Pt interface. However, the $C-V$ measurement voltage was intentionally limited to -5 V (corresponds to 0.6 μm away from Pt) to avoid disturbing the vacancy profile during the measurement. The donor profile between -5 and -35 V (or between 0.6 and 1.2 μm) was not measured experimentally. We can estimate the donor profile in this region by assuming that the plateau in the "initial" profile in Fig. 4(c) has reached the uniform bulk. Therefore, in the region between 0.6 and 1.2 μm, the concentration remains constant and equal to the plateau value. The justification for this assumption is evidenced in the three donor profiles shown in Fig. 3(c). Even though the vacancy-denuded zone expanded deeper into $SrTiO_{3-x}$ with time, the profiles always plateaued at the same concentration.

Integrating the Poisson's equation using the estimated "initial" profile in Fig. 4(b) starting from 1.2 μm yielded the electric field distribution shown in Fig. 4(d). The absolute magnitude of the field's slope remained constant from 1.2 to $\sim$0.5 μm and then decreased toward 0. The change in slope is associated with the donor concentration falling off from the plateau as the Pt interface is approached. The vacancy mobility obtained in this analysis required a position at which both the "initial" and the "5 min" donor profiles have plateaued. Examining Fig. 4(c) reveals that the earliest position where this occurred is approximately 0.6 μm. A 500 kV/cm electric field is associated with the position as indicated by the dotted lines in Fig. 4(d).

In the RS literature, the typical field used to switch a device ranges from 100 kV/cm to 1 MV/cm. For example, 1.5 V dropped uniformly across 30 nm film corresponds to a field of 500 kV/cm. If oxygen vacancy redistribution across 5 nm of an oxide is required to switch the resistance of a thin film device at 500 kV/cm and 300 K, using our experimentally measured mobility, the RS time would be $\sim$1 s. This value is 8 orders of magnitude higher than the reported values for Pt/$SrTiO_{3-x}$[16] and Pt/TiO_{2-x}[7] thin film devices. It is, however, consistent with the switching time found in devices relying on uniform oxygen vacancy motion.[15,32] For example, in the Pt/TiO_{2-x}/Pt thin film system, Strachan *et al.*[11] reported a $\sim$10 ns switching time while Shima *et al.*[15] reported the switching time to be 0.5 s. The distinguishing factor between these two reports is the device's uniformity. For the fast-switch, there was clear evidence that the main current conduction and vacancy migration path was limited to a small filament (0.2×0.3 μm^2) created during electroforming of the much bigger contact (2×2 μm^2). For the slow-switch, the current scaled with contact area (from 20×20 to 60×60 μm^2), indicating a relatively uniform contact.

Electrocoloration experiments on single crystal oxides present another set of studies that estimates uniform oxygen mobility. These monitor electric-field induced, macroscopic motion of a color front from one electrode to another, typically performed at slightly elevated temperatures (<800 K) and under a relatively modest electric fields (<20 kV/cm).[12–14] When extrapolated, the room temperature oxygen vacancy

mobility from electrocoloration measurement, despite the 2 to 3 orders of magnitude variation from report to report, is comparable to the value presented in this article and much too low to explain nanosecond switching.[13,14]

It has been reported that oxygen vacancies can diffuse up to 5 to 6 orders of magnitude faster along dislocations and grain boundaries than through perfect single crystals.[21,33] The dislocation density in our $SrTiO_{3-x}$ crystals was approximately 10^8 cm^{-2} as assessed by etching and electron channeling contrast imaging (ECCI).[34] Therefore, the Schottky depletion region of the diodes investigated here was intersected by 2×10^5 dislocations. Significantly faster oxygen vacancy migration along dislocations could result in fast switching of the $I-V$ behavior while leaving the $C-V$ relatively unchanged. However, no hysteresis was observed during repeated $I-V$ sweeps of the $Pt/SrTiO_{3-x}$ diode, as shown in Fig. 1(b). The forward bias current changed slowly at room temperature [Fig. 2(c)], on the same time scale as the observed changes in $C-V$. The similar rates of change for both $I-V$ and $C-V$ suggest that the bulk and filamentary oxygen vacancy migration rates are similar in the current system. The same conclusion was reached by the authors through the analysis of contrast changes in electron beam induced current (EBIC) measurements of the same $Pt/SrTiO_{3-x}$ system.[35] The EBIC contrast was interpreted as arising from local differences in the Schottky depletion layer width, which relates closely to the near-interface oxygen vacancy concentration. The change in EBIC contrast in response to thermal and electrical stressing occurred slightly faster along dislocations than the bulk crystalline $SrTiO_{3-x}$; The relative difference in magnitude was only 10% to 20%.

A large current density is often a consequence of filamentary conduction. At -1 V, the slow, uniform switch reported by Shima *et al.*[15] had a current density of 3 A/cm^2 while the fast, filamentary switch reported by Strachan *et al.*[11] had a current density of 5×10^5 A/cm^2. Under such a large current density, the local temperature increase due to Joule heating could be as high as 350 °C.[11,36] In this work, the mobility values were obtained at room temperature, as the leakage current during the -35 V stressing was small. Assuming an activation energy of 1 eV, a 300 °C temperature rise is enough to increase the mobility value by more than 8 orders of magnitude, which brings the switching time to below 10 ns. However, at this mobility value, the retention time (the time it takes for oxygen vacancy to diffuse back to the equilibrium profile) remains questionable. Sixteen orders of magnitude difference between 10 ns switching and 10 year retention exists. Through simulation, Noman *et al.*[20] indicated that such a time gap cannot be closed realistically by changing temperature and electric field. An electric field dependent mobility was one mechanism suggested that would introduce a significant nonlinearity into oxygen vacancy mobility. However a field strength of several hundred kV/cm corresponds to an average of only several mV per vacancy jump distance (4 Å in $SrTiO_3$). Such a small voltage is not expected to affect the activation energy for motion, an expectation confirmed by the low value of vacancy mobility measured under an electric field of ~500 kV/cm in this work.

Clear evidence in the literature of an oxygen-migration-based resistive switching device that satisfies all the technological requirements for nonvolatile memory is lacking. Recent modeling and experimental work presented here suggest that the "voltage-time" dilemma cannot be resolved by a combination of Joule heating and typical electric fields used in RS devices. However, the results of modeling apply to a system where only drift and diffusion take place. Since lightly reduced $SrTiO_{3-x}$ does not readily form oxygen deficient second phases (extreme oxygen-deficiency can lead to $SrTiO_{2.5}$,[37] but a vacancy concentration of $1 \times 10^{18}/cm^{-3}$ corresponds to $SrTiO_{2.99994}$), it closely approximates the theoretical system. In many other systems, the equilibration of oxygen vacancy profile is not just the balance between concentration gradient and electric field. For example, it is known that in oxides such as TiO_2 and TaO, oxygen deficient phases can exist in bulk equilibrium with the stoichiometric phase.[18] Filaments of the oxygen deficient Magnéli phase in TiO_2 have been observed to form post electroforming. The subsequent switching is believed to occur as a result of the rupturing and reforming of the Magnéli phase.[11] While inducing phase change via oxygen vacancy redistribution could be a way to resolve the voltage-time dilemma, more information is needed regarding the kinetics of such a process.

IV. SUMMARY AND CONCLUSION

$I-V$ and $C-V$ measurements were performed on high quality $Pt/SrTiO_{3-x}$ and $Pt/Nb:SrTiO_3$ (control sample) diodes having similar doping densities. The electrical characteristics of $Pt/Nb:SrTiO_3$ diodes with immobile donors were insensitive to thermal and electric stresses, while those of the $Pt/SrTiO_{3-x}$ diode with mobile oxygen vacancy donors evolved significantly. The vacancy profile evolution of the diode under 0 and -35 V applied bias were obtained from $C-V$ measurements. The 0 V profile evolution can be the result of either a vacancy pile-up at the Pt interface or an oxidation of the interface by adsorbed oxygen. $C-V$ analysis is unable to determine one from the other. However, its determination is not crucial to the study of vacancy mobility as long as the analysis is limited to region away from the interface. A -35 V stressing was used to affect vacancy profile deeper into the $SrTiO_{3-x}$ crystal. The profile evolution under -35 V applied bias was dominated by drift. From the analysis of the -35 V profile evolution, the oxygen vacancy mobility values of 1.5×10^{-13} cm^2/Vs at room temperature were found for an electric field value of 500 kV/cm. A switching time of 1 s was estimated for typical thin film devices using this mobility value. Such a time scale, while 8 orders of magnitude higher than the nanosecond switches, is consistent with reports of switching based on uniform motion of oxygen vacancies in which the Joule heating effect was small.

ACKNOWLEDGMENTS

This work was in part supported by AFOSR grant FA95501010365, by the Pennsylvania Infrastructure Technology Alliance, and by the Defense Advanced Research

Projects Agency under Grant No. HR0011-06-1-0047 through the Carnegie Mellon MISCIC Center.

[1]R. Waser and M. Aono, Nat. Mater. **6**, 833 (2007).
[2]D. B. Strukov, G. S. Snider, D. R. Stewart, and R. S. Williams, Nature **453**, 80 (2008).
[3]B. H. Calhoun, C. Yu, L. Xin, M. Ken, L. T. Pileggi, R. A. Rutenbar, and K. L. Shepard, P. IEEE **96**, 343 (2008).
[4]A. Chung, J. Deen, J.-S. Lee, and M. Meyyappan, Nat. Nanotechnol. **21**, 412001 (2010).
[5]E. Linn, R. Rosezin, C. Kugeler, and R. Waser, Nat. Mater. **9**, 403 (2010).
[6]S. C. Chae, J. S. Lee, S. Kim, S. B. Lee, S. H. Chang, C. Liu, B. Kahng, H. Shin, D.-W. Kim, C. U. Jung, S. Seo, M.-J. Lee, and T. W. Noh, Adv. Mater. **20**, 1154 (2008).
[7]J. J. Yang, M. D. Pickett, X. Li, A. A. OhlbergDouglas, D. R. Stewart, and R. S. Williams, Nat. Nanotechnol. **3**, 429 (2008).
[8]J. J. Yang, F. Miao, M. D. Pickett, D. A. A. Ohlberg, D. R. Stewart, C. N. Lau, and R. S. Williams, Nat. Nanotechnol. **20**, 215201 (2009).
[9]M. D. Pickett, D. B. Strukov, J. L. Borghetti, J. J. Yang, G. S. Snider, D. R. Stewart, and R. S. Williams, J. Appl. Phys. **106**, 074508 (2009).
[10]D.-H. Kwon, K. M. Kim, J. H. Jang, J. M. Jeon, M. H. Lee, G. H. Kim, X.-S. Li, G.-S. Park, B. Lee, S. Han, M. Kim, and C. S. Hwang, Nat. Nanotechnol. **5**, 148 (2010).
[11]J. P. Strachan, M. D. Pickett, J. J. Yang, S. Aloni, A. L. David Kilcoyne, G. Medeiros-Ribeiro, and R. Stanley Williams, Adv. Mater. **22**, 3573 (2010).
[12]J. Blanc and D. L. Staebler, Phys. Rev. B **4**, 3548 (1971).
[13]R. Waser, T. Baiatu, and K.-H. Härdtl, J. Am. Ceram. Soc. **73**, 1654 (1990).
[14]H. I. Yoo, M. W. Chang, T. S. Oh, C. E. Lee, and K. D. Becker, J. Appl. Phys. **102**, 093701 (2007).
[15]H. Shima, N. Zhong, and H. Akinaga, Appl. Phys. Lett. **94**, 082905 (2009).
[16]D. Choi, D. Lee, H. Sim, M. Chang, and H. Hwang, Appl. Phys. Lett. **88**, 082904 (2006).
[17]W. C. Chien, Y. C. Chen, E. K. Lai, Y. D. Yao, P. Lin, S. F. Horng, J. Gong, T. H. Chou, H. M. Lin, M. N. Chang, Y. H. Shih, K. Y. Hsieh, R. Liu, and L. Chih-Yuan, IEEE Electron Device Lett. **31**, 126 (2010).
[18]J. J. Yang, M.-X. Zhang, J. P. Strachan, F. Miao, M. D. Pickett, R. D. Kelley, G. Medeiros-Ribeiro, and R. S. Williams, Appl. Phys. Lett. **97**, 232102 (2010).
[19]R. Waser, R. Dittmann, G. Staikov, and K. Szot, Adv. Mater. **21**, 2632 (2009).
[20]M. Noman, W. Jiang, P. Salvador, M. Skowronski, and J. Bain, Appl. Phys. A Mater. **102**, 877 (2011).
[21]K. Szot, W. Speier, G. Bihlmayer, and R. Waser, Nat. Mater. **5**, 312 (2006).
[22]M. Janousch, G. I. Meijer, U. Staub, B. Delley, S. F. Karg, and B. P. Andreasson, Adv. Mater. **19**, 2232 (2007).
[23]T. Ohnishi, K. Shibuya, M. Lippmaa, D. Kobayashi, H. Kumigashira, M. Oshima, and H. Koinuma, Appl. Phys. Lett. **85**, 272 (2004).
[24]B. Jalan, R. Engel-Herbert, T. E. Mates, and S. Stemmer, Appl. Phys. Lett. **93**, 052907 (2008).
[25]E. H. Rhoderick, *Metal-Semicondcutor Contacts* (Calrendon Press, Oxford, 1978).
[26]T. Shimizu and H. Okushi, J. Appl. Phys. **85**, 7244 (1999).
[27]R. A. van der Berg, P. W. M. Blom, J. F. M. Cillessen, and R. M. Wolf, Appl. Phys. Lett. **66**, 697 (1995).
[28]J. Maier, *Physical Chemistry of Ionic Materials* (Wiley, New York, 2004).
[29]N. Wakabayashi, M. Takeichi, H. Uchida, and M. Watanabe, J. Phys. Chem. B **109**, 5836 (2005).
[30]T. P. Drüsedau and K. Koppenhagen, Surf. Coat. Technol. **153**, 155 (2002).
[31]R. C. Neville, B. Hoeneisen and C. A. Mead, J. Appl. Phys. **43**, 2124 (1972).
[32]J. R. Jameson, Y. Fukuzumi, Z. Wang, P. Griffin, K. Tsunoda, G. I. Meijer, and Y. Nishi, Appl. Phys. Lett. **91**, 112101 (2007).
[33]K. Szot, W. Speier, R. Carius, U. Zastrow, and W. Beyer, Phys. Rev. Lett. **88**, 075508 (2002).
[34]R. Kamaladasa, W. Jiang, P. A. Salvador, M. Skowronski, and Y. Picard (unpublished).
[35]W. Jiang, D. Evans, J. A. Bain, M. Skowronski, and P. A. Salvador, Appl. Phys. Lett. **96**, 092102 (2010).
[36]Y. M. Lu, W. Jiang, M. Noman, J. A. Bain, P. A. Salvador, and M. Skowronski, J. Phys. D **44**, 185103 (2011).
[37]R. Perez-Casero, Perri, egrave, J. re, A. Gutierrez-Llorente, D. Defourneau, E. Millon, W. Seiler, and L. Soriano, Phys. Rev. B **75**, 165317 (2007).